AD-A272 715

Quarterly Technical Report

Growth, Characterization and Device Development in
Monocrystalline Diamond Films

DTIC
ELECTE
NOV 16 1993
E

R. F. Davis, J. T. Glass, and R. J. Nemanich*
P. K. Baumann*, J. Berhnolc*, T. P. Humphreys*, K. Ishibashi**,
M. T. McClure, N. R. Parikh**, L. Porter, B. R. Stoner,
J. van der Weide*, M. G. Wensell*, and Z. Zhang*
North Carolina State University
c/o Materials Science and Engineering Department
*Department of Physics
**Physics, University of North Carolina-Chapel Hill
Raleigh, NC 27695

September, 1993

93-27560

REPORT DOCUMENTATION PAGE

1. AGENCY USE ONLY (Leave blank)	2. REPORT DATE September, 1993	3. REPORT TYPE AND DATES COVERED Quarterly Technical 7/1/93–9/30/93

4. TITLE AND SUBTITLE

Growth, Characterization and Device Development in Monocrystalline Diamond Films

6. AUTHOR(S)

Robert F. Davis, J. T. Glass and R. J. Nemanich

5. FUNDING NUMBERS

s400003srr14
1114SS
N00179
N66005
4B855

7. PERFORMING ORGANIZATION NAME(S) AND ADDRESS(ES)

North Carolina State University
Hillsborough Street
Raleigh, NC 27695

8. PERFORMING ORGANIZATION REPORT NUMBER

N00014-93-I-0437

9. SPONSORING/MONITORING AGENCY NAMES(S) AND ADDRESS(ES)

Sponsoring: ONR, Code 1513:CMB, 800 N. Quincy, Arlington, VA 22217-5000
Monitoring: Office of Naval Research Resider
The Ohio State University Research Center
1960 Kenny Road
Columbus, OH 43210-1063

10. SPONSORING/MONITORING AGENCY REPORT NUMBER

11. SUPPLEMENTARY NOTES

12a. DISTRIBUTION/AVAILABILITY STATEMENT

Approved for Public Release; Distribution Unlimited

12b. DISTRIBUTION CODE

13. ABSTRACT (Maximum 200 words)

For the heteroepitaxial deposition of diamond films, material selection criteria have been used to choose the closely lattice parameter matched substrate of Cu and the subsequent candidate interlayer materials of Ni, Si and Ti, the latter of which hold promise for both pseudomorphic matching to Cu and the promotion of the high density nucleation of diamond. Initial experiments of the Cu/Ti system have shown that a 20 Å Ti layer can improve the particle density on Cu by nearly a factor of 10. Copper films have been evaporated under UHV conditions for examination as rectifying contacts. Atomic force microscopy indicated island growth of the Cu. Current-voltage measurements and UPS at 293 K revealed rectifying characteristics and a $\Phi \cong 1.1$ eV, respectively. In research regarding the negative electron affinity of the 2×1 diamond (100) surface, theoretical calculations indicate that it is associated with a monohydride terminated surface.

14. SUBJECT TERMS

diamond, nucleation, heteroepitaxial growth, Cu substrates, pseudomorphic interlayers, Cu rectifying contacts, atomic force microscopy, negative electron affinity, monohydride terminated surface

15. NUMBER OF PAGES

32

16. PRICE CODE

17. SECURITY CLASSIFICATION OF REPORT	18. SECURITY CLASSIFICATION OF THIS PAGE	19. SECURITY CLASSIFICATION OF ABSTRACT	20. LIMITATION OF ABSTRACT
UNCLAS	UNCLAS	UNCLAS	SAR

Table of Contents

Accesion For		
NTIS CRA&I	☑	
DTIC TAB	☐	
Unannounced	☐	
Justification		
By		
Distribution /		
Availability Codes		
Dist	Avail and / or Special	
A-1		

DTIC QUALITY INSPECTED 5

I. Introduction

Diamond as a semiconductor in high-frequency, high-power transistors has unique advantages and disadvantages. Two advantages of diamond over other semiconductors used for these devices are its high thermal conductivity and high electric-field breakdown. The high thermal conductivity allows for higher power dissipation over similar devices made in Si or GaAs, and the higher electric field breakdown makes possible the production of substantially higher power, higher frequency devices than can be made with other commonly used semiconductors.

In general, the use of bulk crystals severely limits the potential semiconductor applications of diamond. Among several problems typical for this approach are the difficulty of doping the bulk crystals, device integration problems, high cost and low area of such substrates. In principal, these problems can be alleviated via the availability of chemically vapor deposited (CVD) diamond films. Recent studies have shown that CVD diamond films have thermally activated conductivity with activation energies similar to crystalline diamonds with comparable doping levels. Acceptor doping via the gas phase is also possible during activated CVD growth by the addition of diborane to the primary gas stream.

The recently developed activated CVD methods have made feasible the growth of polycrystalline diamond thin films on many non-diamond substrates and the growth of single crystal thin films on diamond substrates. More specifically, single crystal epitaxial films have been grown on the {100} faces of natural and high pressure/high temperature synthetic crystals. Crystallographic perfection of these homoepitaxial films is comparable to that of natural diamond crystals. However, routes to the achievement of rapid nucleation on foreign substrates and heteroepitaxy on one or more of these substrates has proven more difficult to achieve. This area of study has been a principal focus of the research of this contract.

At present, the feasibility of diamond electronics has been demonstrated with several simple experimental devices, while the development of a true diamond-based semiconductor materials technology has several barriers which a host of investigators are struggling to surmount. It is in this latter regime of investigation that the research described in this report has and continues to address.

In this reporting period, material selection criteria have been used to choose the closely lattice parameter matched substrate of Cu and the subsequent candidate interlayer materials of Ni, Si and Ti, the latter of which held promise for both pseudomorphic lattice matching to Cu and the promotion of the high density nucleation of diamond. In addition, UHV electron beam deposited epitaxial Cu films have been deposited on natural II-b (p-type) diamond (001) substrates. Rectifying characteristics and Schottky barrier height of 1.1 eV were determined. Finally, the previously reported negative electron affinity in the diamond (100) surface has been theoretically shown to be associated with a monohydride terminated surface.

The following subsections detail the experimental procedures for each of the aforementioned studies, discuss the results and provide conclusions and references for these studies. Note that each major section is self-contained with its own figures, tables and references.

II. Use of Interlayers on Cu for Improved Heteroepitaxy

Michael T. McClure, Brian R. Stoner, and Jeffrey T. Glass

A. Introduction

Despite a significant amount of research on the CVD of diamond films, heteroepitaxial growth has been limited by the lack of close lattice-parameter matched substrates. The majority of substrates used for diamond growth have been refractory metals that form a carbide prior to the nucleation of diamond. These materials produce high particle densities, however they have yet to show any epitaxial growth of diamond. Heteroepitaxial diamond crystallites have been produced on c-BN, Si, and Ni substrates [2-4], but monocrystalline films have not been produced. The success of c-BN and Ni substrates most likely came from the low lattice parameter mismatch (1.3% and 1.2%, respectively), while the success of Si, with a 22% lattice parameter mismatch, most likely came from the presence of an SiC interlayer.

This project proposes to use a close lattice-parameter matched substrate, Cu, and evaporate materials that have shown to produce high nucleation densities or heteroepitaxial diamond crystals as an interlayer to promote heteroepitaxial deposits of diamond. The interlayer material will be deposited thin enough to be pseudomorphically matched to copper. This will combine the high nucleation of the interlayer material with the close lattice-parameter match of copper.

B. Experimental Procedure

The material selection criteria for the interlayer materials consisted of four factors: 1) high nucleation density as a bulk substrate; 2) low strain energy density in the interlayer material upon 100% two dimensional matching with the substrate; 3) ease of deposition of the interlayer material; and 4) degree of solubility at growth temperatures. The first step of the material selection process came from the work done by Wolter *et al.* on Si and various refractory materials [5].

The second step of the selection process used a program called ORPHEUS developed by Braun [6, 7]. The program overlays the reciprocal surface nets of the substrate and overlayer candidate material. The user is then interactively aided to match the periodicity of the overlayer surface net and the substrate surface net. The change in the reciprocal lattice vector for the overlayer material is then used to calculate the strain energy density in the overlayer as well as the dislocation density. This computer model is relatively simplistic in that it only considers geometric factors, assumes the overlayer's elastic properties are the same as a bulk sample, and neglects other factors such as bond configurations, interdiffusion, and chemical

3

reactions occurring between the substrate and the overlayer. Nevertheless, this program has successfully predicted the observed heteroepitaxial orientation between diamond and ß-SiC.[8]

Once the candidate materials have been evaluated for their "tendency to yield epitaxy," they were evaluated on the their ease of deposition. The deposition technique was a resistive filament evaporation system connected in-vacuo to the diamond growth CVD chamber and a surface analysis chamber capable of performing Auger electron spectroscopy (AES) and x-ray photoelectron spectroscopy (XPS). The interlayer materials, with the exception of Si, were wrapped around a 0.5 mm W wire and were heated using a Sorensen power supply. (Alternative methods for the evaporation of Si are being pursued.) Deposition rates of the interlayer material are calculated by taking the ratio of the peak area intensity of Cu and the deposited material.[1] This information yields thickness of the deposited material assuming a uniform layer.

Growth of the diamond films used a MWCVD system and the bias enhanced nucleation (BEN) technique. The biasing conditions were a substrate voltage of -250 V and a $CH_4:H_2$ ratio of 5% in a flow rate of 500sccm of H_2. The growth conditions were a $CH_4:H_2$ ratio of 0.2% in a flow rate of 500sccm of H_2 and a growth time of 9 hours. The substrate temperature was dependent on the material system.

C. Results and Discussion

Materials Selection Results. Based upon the results by Wolter *et al.*[5] of a substrate material study using the BEN technique, Si, Ti, and Hf were chosen as potential interlayer materials. The nucleation densities found in that work are shown in Table I. Although not included in the work by Wolter *et al.*, Ni has shown promising potential as a substrate capable of producing heteroepitaxial diamond growth[3] and for that reason Ni was considered for the second stage of the selection process.

Table I. Nucleation of diamond on various refractory substrates
after 60 minutes of biasing at -250V.

Substrate	Nucleation density (cm^{-3})
Si	3×10^{10}
Ti	5×10^{9}
Ta	7×10^{7}
Hf	7×10^{9}

The second stage of the selection process was the two-dimensional matching of the substrate and the candidate interlayer material through the use of the ORPHEUS program.

Those results are summarized in Table II. The strain energy density was lowest for Ni{001} interlayers on Cu{001} surfaces with the next lowest being Ti{0001} interlayers on Cu{111} surfaces. The carbides of the candidate material, where reliable data could be found, is also included because a part of the growth sequence is the formation of a carbide layer prior to diamond formation. For the case of Ti, the best matching occurred when the (0001) plane was parallel to the Cu(111) plane. The best two candidate systems from this stage of the selection process were Ni(001) on Cu(001) and Ti(0001) on Cu(111).

Table II. Interfacial 2-D matching of Cu substrate and candidate interlayer materials. Diamond is added as a reference.

| Interlayer Material | Parallel Planes | | Strains | | | Strain Energy Density $(\times 10^{11}\,erg\,cm^{-3})$ | Misfit Dislocation Spacing (NND) |
	Cu	Interlayer	ε_{xx} %	ε_{yy} %	γ_{xy} %		
Diamond	{001}	{001}	1.2	1.2	0	0.0019	79.6
Ni	{001}	{001}	2.4	2.4	0	0.013	30.1
Ti	{100}	{0001}	25.6	2.6	39.9	1.16	2.7
TiC	{001}	{001}	16.3	16.3	0	1.12	4.7
Ti	{111}	{0001}	9.59	9.59	0	0.14	18.3
TiC	{111}	{111}	16.3	16.3	0	1.2	6.8
Si	{001}	{001}	33.5	33.5	0	2.0	1.7
SiC	{001}	{001}	17.2	17.2	0	1.1	3.9
Ta	{001}	{001}	9.2	9.2	0	0.19	8.4
TaC	{001}	{001}	19.0	19.0	0	2.0	3.9

The third step in the selection process was ease of deposition for the resistive filament evaporation system. The primary concern for this step was the melting temperature of the material to be evaporated. A lower melting temperature was preferred because less power will be required to deposit the material and the lifetime of the resistive filament will be extended. Listed in Table III are the melting temperatures of the materials under consideration with W included because it is the resistive filament material. From this step, Hf and Ta were less desirable than the others because the temperature needed to evaporate Hf and Ta may also cause contaminating evaporation from the W filament.

The fourth step was to consider the degree of solubility of the candidate material in Cu at typical growth temperatures. Listed in Table IV is the maximum solubility of the materials in Cu and the temperature at which maximum solubility occurs. Examination of Table IV indicates that solid solution formation is possible for all the materials especially when one remembers that only small amounts of the material will be used to form the interlayer.

Table III. Table of melting temperatures of candidate interlayer materials [9].

Interlayer Material	Melting temperature (°C)
Hf	2231
Ni	1455
Si	1414
Ta	3020
Ti	1670
W	3680

Table IV. Table of solubility of candidate materials in Cu and temperature of maximum solubility.[10]

Element	Weight percent solubility in Cu (wt% Cu)	Temperature of maximum solubility (°C)
Ni	100	>354.5
Si	94.6	850
Ti	94	885

The final consideration revealed that Ni will almost instantaneously form a solid solution for reasonable growth temperatures. Based on the results of the first three steps in the selection process, Ni, Si, and Ti appear to be the most promising materials as interlayers. The fourth step revealed the need to find a method(s) to kinetically limit the formation of a solid solution between the Cu and the interlayer material. One method will be to carburize the interlayer quickly to limit interdiffusion. Because Ni does not form a stable carbide, another method is needed. However, Yang et al.[3] showed that the formation of a hydride of Ni was the technique needed to form epitaxial diamond and a method similar to theirs will be used in this work.

Experimental Results. As a result of the material selection process, Ti was chosen as the first material to be used as an interlayer because of its ease of deposition. Three thicknesses and bias times were chosen as "proof-of-concept" conditions and the resulting particle densities are shown in Table V. Wolter et al.[5] reported a particle density on Cu of 1×10^6 cm^{-2} after 90 minutes of biasing. Examination of the data in Table V reveals that the bias time can be drastically reduced to 5 minutes and the particle density can be increased to 7×10^6 cm^{-2} with a 20Å Ti interlayer.

Table V. Table of particle densities for the Cu/Ti substrate/interlayer system.

Thickness (Å)	Bias Time (min.)	Particle density (cm^{-2})
5	0	1×10^5
10	2	1×10^6
20	5	7×10^6

D. Conclusions

The material selection process revealed that Ni, Si, and Ti are the three most promising materials based on their high nucleation densities as a bulk material, ease of deposition as a thin film, and "tendency to yield epitaxy" on a Cu substrate. In addition, Ni and Si have demonstrated the ability to produce heteroepitaxial diamond crystals under the proper conditions. For the initial experiments, the XPS surface analysis technique has been used to determine the thickness of the interlayer material and the BEN technique has been used to increase the particle density on Cu by nearly an order of magnitude.

E. Future Research Plans and Goals

The future direction of this research plan is to determine the optimum conditions of the BEN technique for the Ti interlayer and to continue investigation of the other two candidate materials. Based on the results using polycrystalline Cu substrates, the focus will be narrowed to using the best material on single crystal Cu substrates.

F. References

1. C. S. Fadley, R. J. Baird, W. Seikhaus, T. Novakov and S. A. L. Bergstrom, Journal of Spectroscopy, 4 93 (1974).

2. M. Yoshikawa, H. Ishida, A. Ishitani, T. Murakami, S. Koizumi and T. Inuzuka, Appl. Phys. Lett., 57 428 (1990).

3. P. C. Yang, W. Zhu and J. T. Glass, J. Mater. Res., 8 1773 (1993).

4. B. R. Stoner and J. T. Glass, Appl. Phys. Lett., 60 698 (1992).

5. S. Wolter and J. T. Glass, presented at ECS Spring Meeting, Honolulu, Hawaii, 1993, The Electrochemical Society, in press.

6. M. W. H. Braun, D. Sc. Thesis, University of Pretoria, South Africa, 1987.

7. M. W. H. Braun and J. H. van der Merwe, S. African J. Sci, 84 670 (1988).

8. W. Zhu, X. H. Wang, B. R. Stoner, G. H. M. Ma, H. S. Kong, M. W. H. Braun and J. T. Glass, Phys. Rev. B, 47 6529 (1993).

9. *CRC Handbbok of Chemistry and Physics*. 73 edn., D.R. Lide, Ed., 1992, CRC Press: Boca Raton, FL.

10. *Alloy Phase Diagrams*, ASM International, H. Baker, Ed., Materials Park, OH, 1992.

III. Epitaxial Cu Contacts on Semiconducting Diamond

P. K. BAUMANN, T. P. HUMPHREYS , R. J. NEMANICH

Department of Physics, North Carolina State University, Raleigh, North Carolina 27695-8202

K. ISHIBASHI, N. R. PARIKH

Department of Physics, University of North Carolina, Chapel Hill, North Carolina 27599-3255

L. M. PORTER, R. F. DAVIS

Materials Science and Engineering Department, North Carolina State University, Raleigh, North Carolina 27695-7907

ABSTRACT

In this study Cu films of 30 nm and 200 nm thickness have been grown on natural type IIb semiconducting diamond C(001) substrates by electron-beam evaporation at 500 °C in UHV. As evidenced by Rutherford backscattering (RBS)/channeling techniques and *in-situ* low-energy electron diffraction (LEED), the as-deposited layers were shown to be epitaxial, with $\chi_{Cu} = 49\%$. In addition, the technique of atomic force microscopy (AFM) has demonstrated island morphology, indicative of 3-dimensional (3D) growth. Moreover, the Cu films displayed excellent adhesion properties with the underlying diamond substrate. Corresponding current-voltage (I-V) measurements conducted at room temperature have shown rectifying characteristics. In addition, a Schottky barrier height of $\Phi_B \cong 1.1$ eV has been determined from ultraviolet photoemission spectroscopy (UPS).

INTRODUCTION

There is a significant scientific and technological interest in the fabrication of rectifying and ohmic contacts for future diamond-based electronic devices. In particular, metal, silicide and semiconductor contacts have been investigated [1, 2, 3]. Recent publications have established excellent mechanical adhesion for polycrystalline Si and SiGe contacts [2, 3]. To date, the majority of rectifying metal contacts exhibit polycrystalline morphology and appear to have poor adhesion properties [1]. In contrast, Ni is the only epitaxilally grown metal contact on diamond exhibiting rectifying behavior at both room- and elevated temperatures [4]. In this study Cu has been selected as a suitable contact metal, since Cu has a near-lattice match to diamond similar to

Ni. Furthermore, no stable Cu carbides exist in the binary Cu-C phase diagram [5]. Therefore Cu is expected to form a physically and chemically abrupt interface with diamond.

In this paper we report the first results regarding hetero-epitaxially grown Cu films on diamond. The microstructure and electrical characteristics for these contacts are presented.

EXPERIMENTAL DETAILS

Several (3x3 and 4x4 mm) natural type IIb semiconducting diamond C(001) crystals (supplied by D. Drucker & ZN.N.V.) were used in this study. Two independent chemical cleaning processes were employed to remove the non-diamond carbon from the surface of the diamond substrates. The first approach was a conventional chemical clean using chromic acid ($CrO_3:H_2SO_4$) (boiling for 15 min), aqua regia (3HCl:1HNO$_3$) (boiling for 15 min) followed by deionized (DI) water (rinsing). The other procedure involved an electrochemical etch [6]. Herefore the samples were mounted on a teflon^{tm} holder and placed between two Pt electrodes in DI water as electrolyte. A DC-voltage of 350 V was applied between the two electrodes. Typical etch times were 3 hours. To assess and compare the effectiveness of these two cleaning processes *in situ* low-energy diffraction (LEED) was used. A comparable unreconstructed (1x1) LEED pattern was observed from crystals cleaned by either approach. Following chemical cleaning the diamond crystals were blown dry with N_2 and mounted on a Mo sample block and transferred into the vacuum system. In order to desorb adsorbed gas contaminants all samples were annealed to 750°C for 15 minutes in ultra-high vacuum (UHV). Prior to growth 5.0 nm of Cu was evaporated from the solid source to liberate any foreign material which may have collected on its surface between depositions. Both large area films and contacts (625 μm in diameter) were grown by electron-beam evaporation. The contact dots were fabricated by employing a Mo shadow mask.

Two independent growth chambers were employed. One system had a base pressure of ~ 5×10^{-9} Torr and featured a Thermionics, model 100-0010, single source evaporator. Due to the small dimensions of this deposition chamber the pressure rose to ~ 2×10^{-7} Torr during growth. In this system, Cu layers of 30 nm and 200 nm thickness were deposited on substrates that were chemically cleaned by chromic acid. A deposition rate of 2.0 - 2.5 nm/min was used. The second chamber (base pressure ~ 1-2 x 10^{-10} Torr) was equipped with a dual source, 270° HM^2 evaporator made by Thermionics. To commence the deposition a deposition rate of 1.0 - 1.2 nm/min. was stabilized, and the shutter was removed from the front of the sample. After 20 nm was deposited, the rate was increased to 2.5 - 3.0 nm/min to give a final thickness of 200 nm. Electrochemically etched crystals were used here. Throughout the deposition (pressure ~

3×10^{-4}) the substrate was rotated to ensure uniform thickness across the sample. In both experiments a growth temperature of 500°C was used and the thickness of the Cu layers was determined by a quartz crystal oscillator.

Several techniques were employed to analyze the samples including *in situ* low-energy diffraction (LEED), Rutherford backscattering (RBS)/channeling, atomic force microscopy (AFM) and current-voltage (I-V) measurements.

RESULTS AND DISCUSSION

The technique of LEED was employed to establish that the as-deposited films were epitaxial as shown in Fig. 1a. In particular, an unreconstructed (1x1) LEED pattern was seen from the as-annealed C(001) substrates (Fig. 1b). This (1x1) pattern was retained after Cu deposition. RBS/channeling has been performed using 2 MeV He^+ ions with a scattering angle of 110°. This gave a depth resolution of 6.7 nm for the Cu film. As shown in Fig. 2, the epitaxial quality of the Cu films grown under higher pressure (2×10^{-7} Torr) has been determined by channeling along the <110> directions of the diamond substrate. χ_{min} is the ratio of the aligned to nonaligned backscattering ion yields and gives the degree of crystallinity for the sample. Values of $\chi_{Dia} = 33$ % and $\chi_{Cu} = 49\%$ have been established for the diamond substrate and the overgrown Cu film, respectively. Furthermore, RBS analysis has shown the presence of oxygen impurities in these Cu films (peak near 950 keV). In addition the random spectrum shows a step in the carbon signal at 760 keV, indicating a non uniform thickness of the Cu layer. The value of χ_{Cu} appears to be fairly high. But considering χ_{Dia}, the crystalline quality of the Cu film is actually quite reasonable.

The non uniformity in the deposited Cu layers has been attributed to island morphology for all samples as evidenced by AFM. The samples grown in a vacuum of 2×10^{-7} Torr exhibited well separated islands. For the Cu contacts of 30 nm thickness oriented islands of ~ 50 nm were observed. However, films of 200 nm thickness grew as well defined islands of ~ 1000 nm x 500 nm in size with smooth morphologies, as shown in Fig 3a. These islands were found to be oriented in the <110> crystallographic directions. Therefore, coalesation of these islands was evident for increasing Cu coverage. However, no continuous layer was formed. Electrical measurements for these samples showed a lack of current transport across one Cu dot. This interesting phenomenon may be attributed to the observed islanding behavior of these Cu films. In comparison, AFM images of the 200 nm thick Cu films deposited under better vacuum (3×10^{-4} Torr) showed a fairly smooth and contiguous surface structure. However, the presence of numerous pinholes was observed (Fig. 3b). Corresponding I-V measurements between a dot

and a large area back contact showed rectifying behavior . In addition, a reverse bias leakage current of ~ 40 nA was observed at 5 V as shown in Fig. 4. This corresponds to a current density of 13×10^{-6} A/cm^2. To remove any highly conductive surface contaminants that could contribute to the reverse bias leakage current, another electrochemical etch was employed. Prior to etching the Cu dots were covered with wax while the diamond surface was kept exposed. Following the etch process the wax was readily removed with acetone. Indeed, in separate experiments investigating electrochemical etching it has been demonstrated that besides graphite also various metals could be removed from the surface by this etching process [7, 8]. However, the I-V characteristics remained unchanged. Therefore it is reasonable to conclude that non diamond carbon and possible metal contaminants have been effectively removed from the diamond surface already in the first place. Consequently, the observed turn-on voltage and corresponding leakage current are believed to be intrinsic to the Cu/C(001) interface. However it will have to be established why Cu contacts display such a high reverse leakage current. Indeed, further studies are necessary to investigate the Cu/diamond interface structure.

Because of the nonlinearity in the semi-logarithmic I-V plot, an independent method to measure the Schottky barrier height Φ_B had to be employed. A value of $\Phi_B \cong 1.1$ eV has been established from ultraviolet photoemission spectroscopy (UPS). Furthermore, the UPS spectra showed that deposition of Cu on diamond C(001) induced a negative electron affinity (NEA) on the surface [9].

It is reasonable to assume that these observations are due to a 3-dimensional (3D) growth mechanism featuring larger nucleation area and better coalesation of the islands compared to the samples deposited under higher pressure. As shown in Fig 2, RBS/channeling clearly demonstrated the presence of oxygen impurities in latter films. The oxygen contamination is expected to be lower for the system with better vacuum. Therefore samples deposited under lower pressure are expected to exhibit better microstructure. No significant effect on the morphology of the Cu films is expected due to the two different chemical cleaning procedures since they appear to be comparable. Therefore it is reasonable to conclude that the differences in microstructure for the epitaxial Cu layers were mainly due to a change in oxygen contamination. Further improvement pertaining to a more uniform growth however, could be accomplished by using higher deposition rates. Also, a higher substrate temperature should increase the surface mobility of Cu on diamond and result in smoother epitaxial layers. With respect to the reports on Ni, even 2-dimensional (2D) growth could be possible [4]. This needs to be object of future work.

Consistent results from all samples clearly indicated that various processing steps including thermal annealing, electrical probing and ultrasonic cleaning did not degrade the excellent mechanical adhesion of the Cu contacts with the underlying diamond substrates.

CONCLUSIONS

Epitaxial Cu films have been deposited on p-type semiconducting natural diamond C(001) substrates using electron-beam evaporation techniques. For all samples 3-dimensional (3D) growth has been observed. However, differences in the nucleation area and the degree of coalesation for the Cu islands have been correlated to the quality of vacuum in the UHV growth chamber. Excellent mechanical adhesion properties have been established for the Cu films throughout. I-V measurements showed rectifying behavior at room temperature. Furthermore, a Schottky barrier height of $\Phi_B \cong 1.1$ eVhas been determined by means of UPS . Suggestions regarding future work to further assess and improve microstructure as well as electrical behavior have been made.

ACKNOWLEDGMENTS

REFERENCES

1 K. Das, V. Venkatesan, K. Miyata, D. L. Dreifus and J. T. Glass, Thin Solid Films, 212 (1992) 19-24

2 V. Venkatesan, D. G. Thompson and K. Das, Symp. Mater. Res. Soc. 270 (1992)

3 T. P. Humphreys, P. K. Baumann, K. F. Turner, R. J. Nemanich, R. G. Alley, D. P. Malta and J. B. Posthill, accepted for publication in the Proceed. 3rd. Internat. Conf. Symp. on Dia. Mat., Honolulu, Hawaii, May, 1993

4 T. P. Humphreys, J. V. La Brasca, R. J. Nemanich, K. Das and J. B. Posthill, Jpn. J. Appl. Phys. 30 (1991) L1409

5 Binary Alloy Phase Diagrams, ed. T. B. Massalski (American Society for Metals, Metals Park, OH, 1990) Vol. 1, p. 839

6 M. Marchywka, P. E. Pehrsson, S. C. Binari, and D. Moses, J. Electrochem. Soc., Vol. 140,
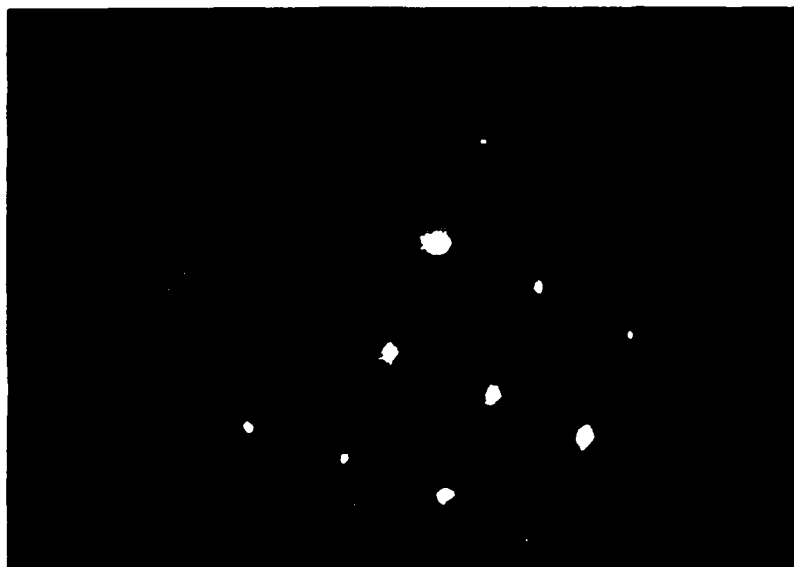
No. 2 (1993)

7 M. Marchywka, private communication (1993)

8 P. K. Baumann, T. P. Humphreys, R. J. Nemanich, to be published (1993)

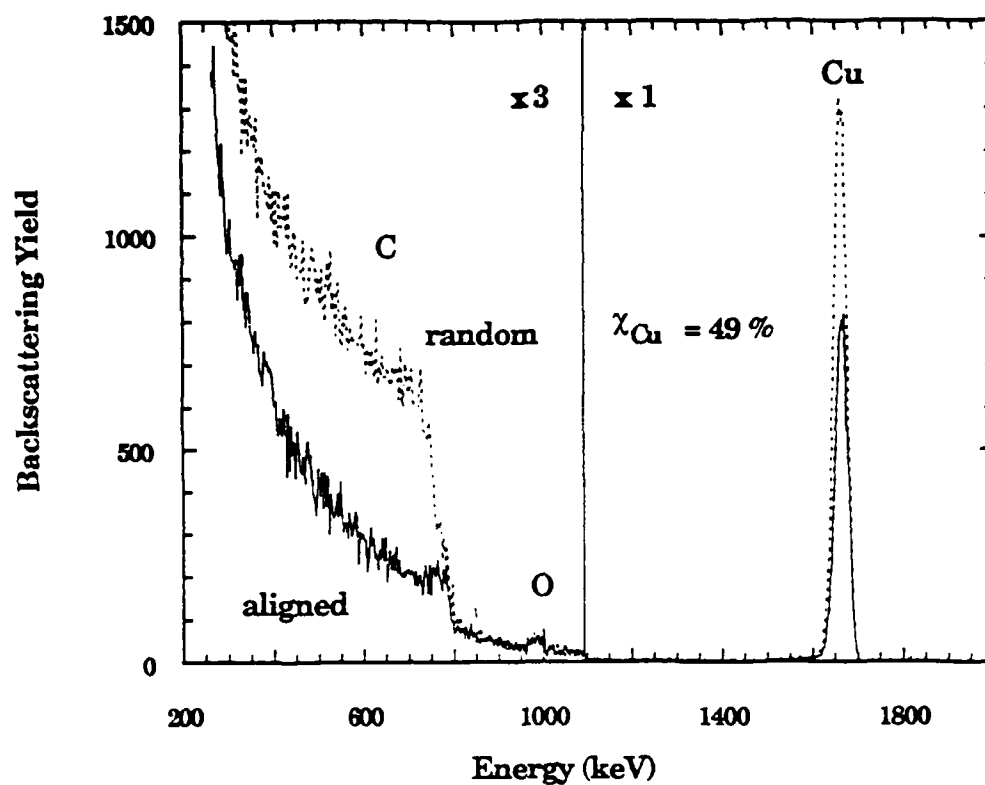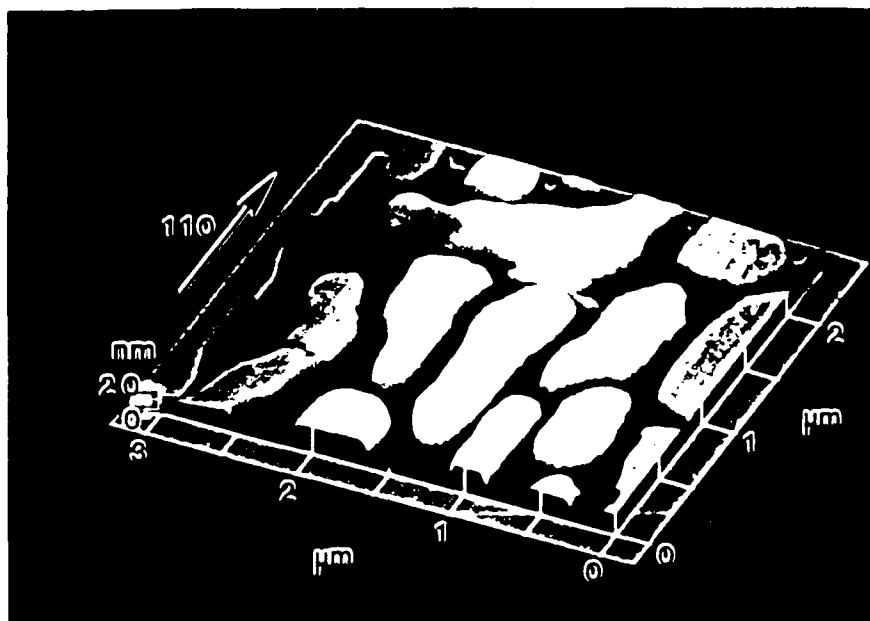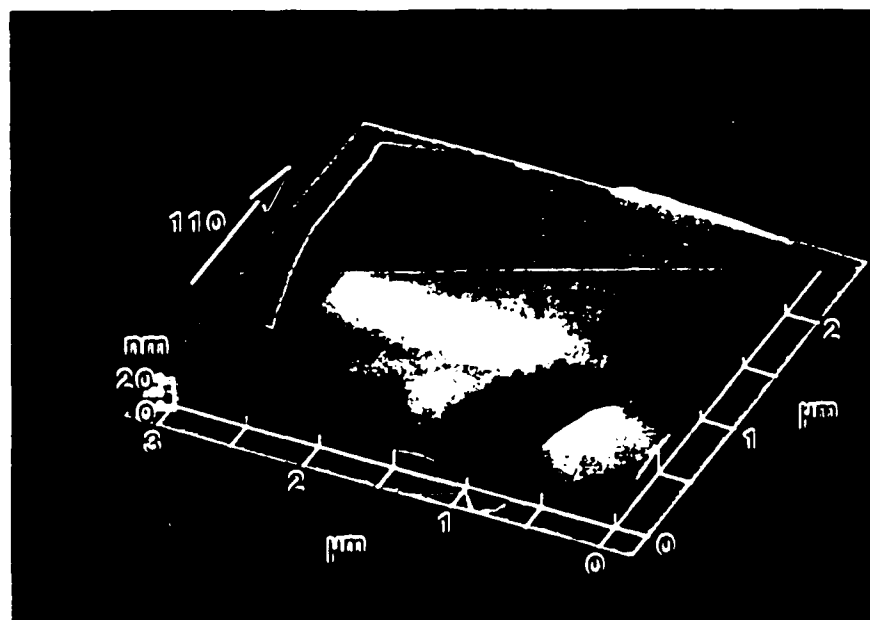9 P. K. Baumann, T. P. Humphreys, R. J. Nemanich, to be published (1993)

Fig. 2. RBS/channeling aligned (solid line) and random (dashed line) spectrum for Cu (001) grown on C(001) substrates (cleaned by $CrO_3 + H_2SO_4$ and $3HCl + 1HNO_3$) in UHV: 2×10^{-7} Torr during growth.

a) Micrograph of 2 μm thick, epitaxial, n-type, device type layer on H₂SO₄ and HCl-HNO₃ and HF, 2x ... ion beam grown

b) Micrograph of 3 μm thick, epitaxial, n-type, device type layer on HF ... ion beam grown
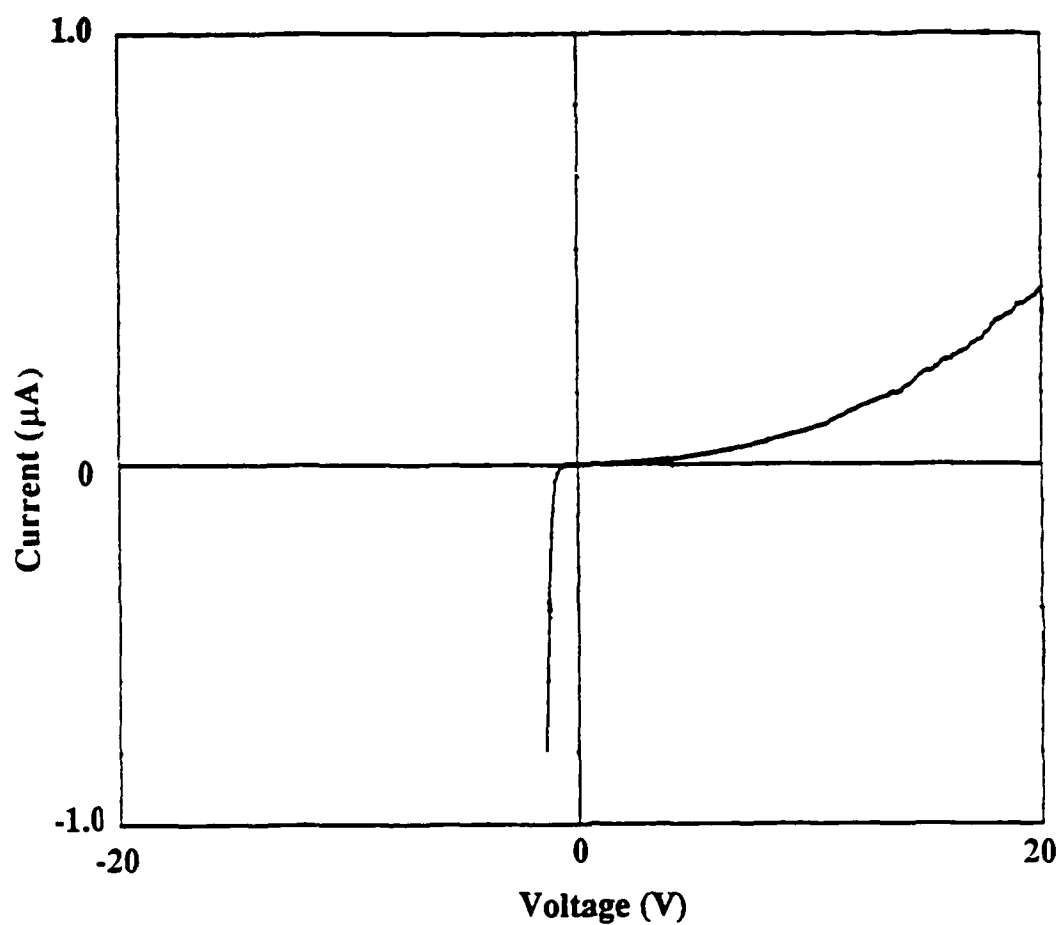
Fig. 4. Linear plot of the room temperature I-V characteristics of heteroepitaxial Cu contacts deposited on type IIb C(001) substrates in 3×10^{-8} Torr.

IV. Negative Electron Affinity Effects on the Diamond (100) Surface

J. van der Weide, Z. Zhang, P. Baumann, M.G. Wensell, J. Bernholc and R.J. Nemanich

Department of Physics and Department of Materials science and Engineering,

North Carolina State University,

Raleigh, North Carolina 27695-8202

Abstract

A negative electron affinity was found for the 2x1 reconstructed diamond (100) surface. Theoretical calculation indicated that the observed negative electron affinity is associated with a monohydride terminated surface. Several methods to obtain a negative electron affinity on the (100) surface are discussed.

Negative electron affinity (NEA) surfaces are semiconductor surfaces which have a work function such that the vacuum level lies below the conduction band edge. Electrons that are present in the conduction band can therefore readily escape the surface. These NEA surfaces are used in a number of applications such as photocathodes, secondary electron emitters and cold-cathode emitters. Current commercial devices are mainly based on GaAs and other III-V semiconductors. These semiconductors are coated with a monolayer of cesium or oxygen-activated cesium to lower the work function of the surface and to obtain a NEA. The work function lowering depends strongly on the amount and activation of the cesium layer and is readily affected by high temperatures, high currents and desorption of cesium under ultra-high vacuum (UHV) conditions. This in turn affects the stability, the life time and the range of operating conditions of these devices.

It has been shown that a stable NEA exists on the diamond (111) surface [1]. However, current diamond deposition techniques to grow high quality diamond films result in (100) oriented surfaces. We have investigated the possibility of inducing a NEA on the diamond (100) surface and report several surface preparation methods which result in a NEA effect on the diamond (100). Theoretical calculations were used to correlate possible surface structures to the observed NEA effect.

The NEA on the diamond (111) surface is associated with the presence of hydrogen bonded to the surface [2, 3]. This monohydride passivated surface is stable in air and can withstand temperatures up to ~1000°C in UHV. At higher temperatures the hydrogen evolves and the surface to change to a positive electron affinity. The free diamond (100) surface has two unsatisfied bonds which would in principle allow the formation of a dihydride terminated surface. Theoretical calculation indicate, however, that the dihydride terminated surface is energetically unfavorable due to the steric repulsion of the hydrogen atoms [4-6]. It is uncertain, therefore, that a stable dihydride terminated surface can be achieved. Theoretical calculations indicate that the

monohydride terminated C(100)-2x1:H surface has a lower energy than the hydrogen-free C(100)-2x1 and the dihydride terminated C(100)-1x1:2H surfaces [4-6]. A 2x1 reconstructed surface can be obtained by annealing the diamond (100) surface to ~1000°C. The 2x1 reconstructed (100) surface is also observed to occur under typical CVD diamond growth conditions, which consist of growth temperatures ranging from 700°C to 1000°C while exposed to a hydrogen rich environment. This surface is therefore presumed be a monohydride terminated surface. This C(100)-2x1 reconstruction is found to be stable in air [7].

Photoemission can be used to determine the presence of a negative electron affinity. Electrons are excited in the photoemission process from the valence band into various conduction band energy levels. A number of these excited electrons will lose energy through inelastic collision processes and accumulate in the energy levels at the conduction band minimum. At a NEA surface the vacuum level lies below the conduction band and electrons from the conduction band can be emitted into the vacuum. When the electrons that have accumulated at the conduction band minimum reach a NEA surface they are emitted and appear in the photoemission spectra as a sharp peak at low electron energies. The position of the peak can be correlated to other features in the photoemission spectra to verify that the emission originated from the conduction band minimum. Auger electron spectroscopy (AES) and low-energy electron diffraction (LEED) were used to determine the chemical composition and the structure of the surface.

Natural diamond wafers with a (100) surface orientation were polished with diamond grit, etched in chromic acid and *aqua regia* and introduced into the vacuum system. The wafers were type IIb (p-type semiconducting) with resistivities on the order of 10^3–10^4 Ωcm and measured $3 \times 3 \times 0.5$ mm^3. Photoemission was excited with monochromatic 21.21 eV light from a helium discharge lamp. Photoemission spectra, shown in Fig. 1, were obtained after the diamond surface had been annealed to

21

temperatures ranging from 545°C to 1070°C. The spectra exhibited random shifts on the order of 0.2 eV with respect to each other possibly due to charging effects. The spectra were therefore aligned according to a bulk feature indicated by the line in Fig 1 to allow comparison between the spectra. As can be seen in the figure, the low energy onset of the spectra shifts by as much as 1 eV towards lower energies as the annealing temperature is increased. This is indicative of a lowering of the work function of the surface since electrons with lower energies are able to escape the surface. After a 1035°C anneal the spectrum exhibits a peak at low energies which becomes more pronounced after a 1070°C anneal. As mentioned above, the appearance of the peak indicates that the work function is such that the vacuum level lies below the conduction band edge and that the surface has a negative electron affinity. The peak is positioned ~7.5 eV below the bulk feature indicated by the solid line. An identical peak at ~7.5 eV below the bulk feature indicated by the solid line can be observed in spectra of NEA diamond (111) surfaces [8-10]. The appearance of the peak on the (100) surface coincided with the appearance of a 2x1 surface reconstruction.

Auger electron spectra, shown in Figure 2, indicate the presence of oxygen on the as-loaded surface which remained present after various anneals ranging from 500°C to 900°C. A reduction in the oxygen signature was observed after repeated anneals to 900°C. No oxygen could be detected after the diamond had been annealed to 1050°C. The surface was observed to transform from a 1x1 structure to a 2x1 structure which coincided with the removal of oxygen from the surface. The presence of hydrogen on the 1x1 and 2x1 surfaces can not be determined from these measurements since AES is not sensitive to hydrogen. However, since no special efforts were made to obtain a strictly oxygen terminated surface it is to be expected that hydrogen is also present on the surface.

The electron affinities of hydrogen-free and monohydride terminated, 2x1 reconstructed diamond surfaces were calculated using the Local Density Approximation

(LDA) and the Car-Parrinello formalism [11]. The hydrogen-free (100) surface was modeled by a supercell consisting of slabs of ten layers of diamond with twelve carbon atoms on each layer. The slabs were separated by 10 Å of vacuum. One hydrogen atom was attached to every surface carbon atom to model the monohydride surface. Due to the supercell size only Γ point sampling was used. Starting from an estimated structure the zero temperature geometry was obtained by steepest descend and/or fast-relax of ion methods [11]. The vacuum level of the surface was determined from the plane-averaged self-consistent potential in the vacuum region. The electron affinity is found as the difference between the vacuum level and the conduction band minimum. However, the position of the conduction band minimum could not be calculated directly since the LDA does not give an accurate solution for unoccupied energy levels. The position of the conduction band minimum was therefore determined by adding the experimental value for the bandgap (5.47 eV) to the position of the valence band maximum. The position of the valence band maximum was found by adding 25.84 eV to the average self-consistent potential inside the slab. This value is the energy difference between the average self-consistent potential in the bulk and the highest occupied energy level and was found in calculations for bulk diamond.

In the calculations the monohydride terminated surface relaxes to a 2x1 reconstructed surface. The plane averaged pseudopotentials for this surface as a function of the distance to the surface are shown in Fig 3. As can be seen in the figure, the effective potential has flattened out in the vacuum region which indicates that the slab separation used in the calculation is sufficiently large to avoid interactions between the slabs. The flat region is representative of the vacuum level. The conduction band minimum is found at 2.0 eV above the vacuum level, resulting in a 2 eV negative electron affinity for C(100)-2x1:H surface. The bare C(100) surface also relaxed to a 2x1 reconstruction in a similar geometry obtained by other authors [12, 13]. Substantial displacements from the ideal bulk positions were found in the surface layers. The plane-

averaged self-consistent potential for this surface is also shown in Fig 3. A 0.44 eV positive electron affinity was found for this surface. Occupied surface states were found inside the band gap near the valence band maximum in agreement with photoemission studies [14]. These states are related to dangling bonds orbitals on the dimer atoms. The electronic charge in these dangling orbitals results in a stronger dipole layer at the bare surface in comparison to the hydrogenated surfaces. The difference in work function and electron affinities between these two surfaces is attributed to this dipole layer.

The CVD grown diamond (100) surface is known to exhibit a 2x1 reconstruction, which has been shown to be stable in air [7]. This 2x1 reconstruction is associated with the presence of a monohydride structure [4-6]. Based on the results described above it is expected that this growth surface would exhibit a NEA. Diamond was deposited on a (100) oriented, type IIb wafer, resulting in a homoepitaxially grown film. After transport in air a faint pattern associated with the 2x1 reconstruction could be discerned. The film was etched to remove a dark discoloration which was due to the deposition process. After the etch the 2x1 reconstruction could not be discerned. However, photoemission spectra, shown in Fig. 4, exhibited a clear peak at 7.3 eV below the bulk feature indicating the presence of a negative electron affinity. This result indicates that the (100) oriented growth surface will exhibit a NEA effect.

Typical diamond growth conditions consist of surface temperatures ranging from 700°C to 1000°C and exposure to a hydrogen plasma with a small (< 5%) amount of a carbon containing gas mixed in. Natural diamond wafers were exposed to a pure hydrogen plasma while heated to 350°C and 500°C to emulate growth conditions. It was found that under these conditions a NEA could be induced.

In summary, a negative electron affinity was obtained on the diamond (100) by annealing a polished and chemically cleaned surface to ~1000°C. This resulted in the desorption of oxygen and the appearance of a 2x1 reconstruction. Theoretical calculations indicate that the negative electron affinity is associated with a monohydride

24

terminated surface. It was found that CVD grown diamond film, which results in a similar surface structure, exhibits a NEA. It was found that a NEA can be also be induced by exposing a heated surface to a hydrogen plasma.

References

1. F.J. Himpsel, J.A. Knapp, J.A. van Vechten and D.E. Eastman, Phys. Rev. B **20**, 624 (1979).
2. B.B. Pate, Surf. Sci. **165**, 83 (1986).
3. B.B. Pate, M.H. Hecht, C. Binns, I. Lindau and W.E. Spicer, J. Vac. Sci. Technol. **21**, 364 (1982).
4. Y.L. Yang and M.P. D'Evelyn, J. Am. Chem. Soc. **114**, 2796 (1992).
5. Y.L. Yang and M.P. D'Evelyn, J. Vac. Sci. Technol., A. **10**, 978 (1992).
6. Y.L. Yang, L.M. Struck, L.F. Sutcu and M.P. d'Evelyn, Thin Solid Films **225**, 203 (1993).
7. T. Tsuno, T. Imai and Y. Nishibayashi, Jap. J. Appl. Phys. **30**, 1063 (1991).
8. J. van der Weide and R.J. Nemanich, submitted to J. Appl. Phys.
9. J. van der Weide and R.J. Nemanich, J. Vac. Sci. Technol. B **10**, 1940 (1992).
10. J. van der Weide and R.J. Nemanich, Appl. Phys. Lett. **62**, 1878 (1993).
11. R. Car and M. Parrinello, Phys. Rev. Lett. **55**, 2471 (1985).
12. S.P. Mehandru and A.B. Anderson, Surf. Sci. **248**, 369 (1991).
13. S. Yang, Private Communication (1993).
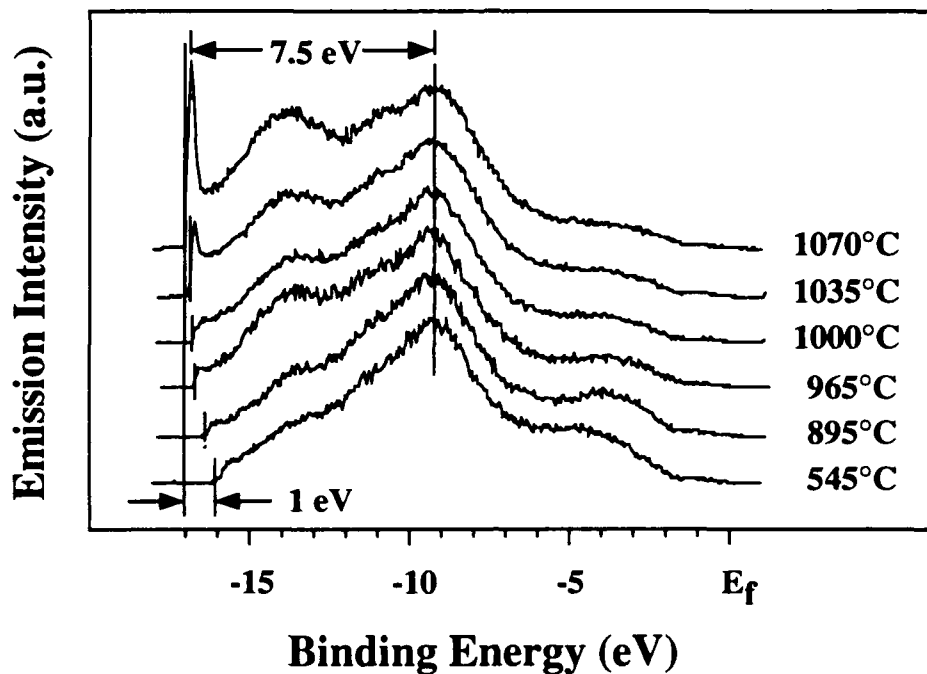14. A.V. Hamza, G.D. Kubiak and R.H. Stulen, Surf. Sci. **237**, 1 (1990).

Fig. 1. Photoemission spectra showing the effects of annealing on the diamond (100) surface. The shift in the back edge is indicative of a lowering of electron affinity and is associated with a transformation from a 1x1 to a 2x1 reconstructed surface. The spectra have been lined up according to peak at ~9 eV below the Fermi level.
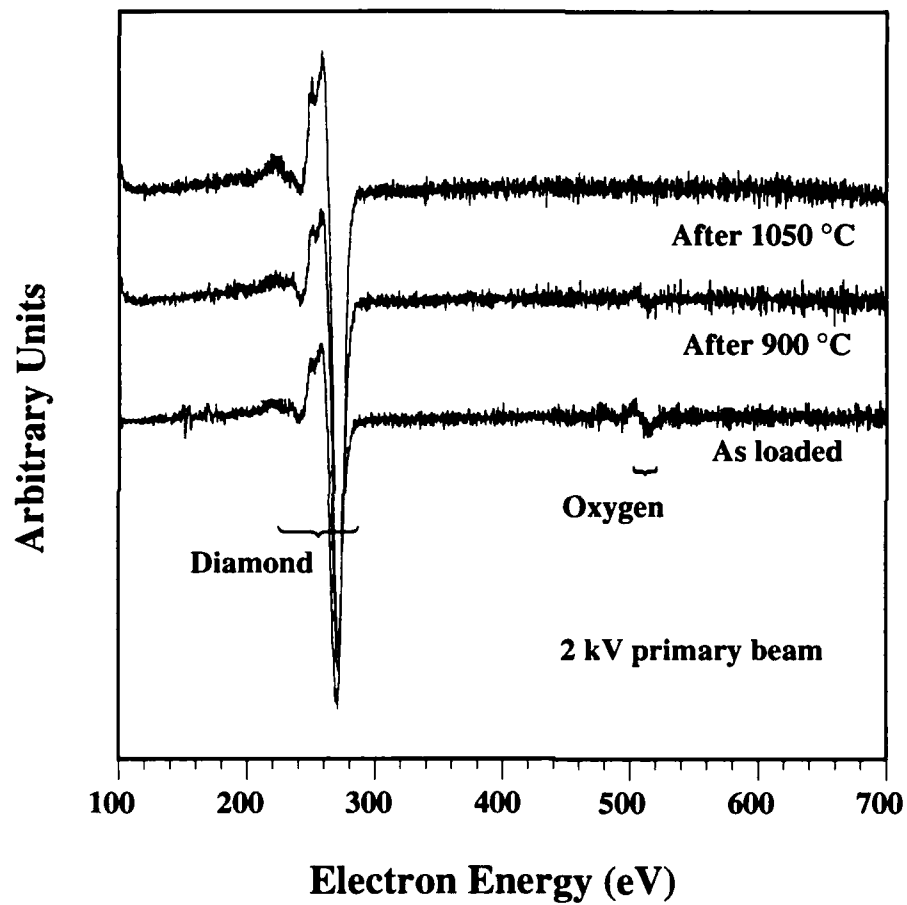
Fig. 2. Auger spectra, obtained from the diamond (100) surface, as a function of annealing temperature. Oxygen, which is present on the surface after sample preparation, is observed to evolve at ~900°C, and removed after a 1050°C anneal. The removal of oxygen coincides with the transformation of the surface from a 1x1 to a 2x1 reconstructed surface.
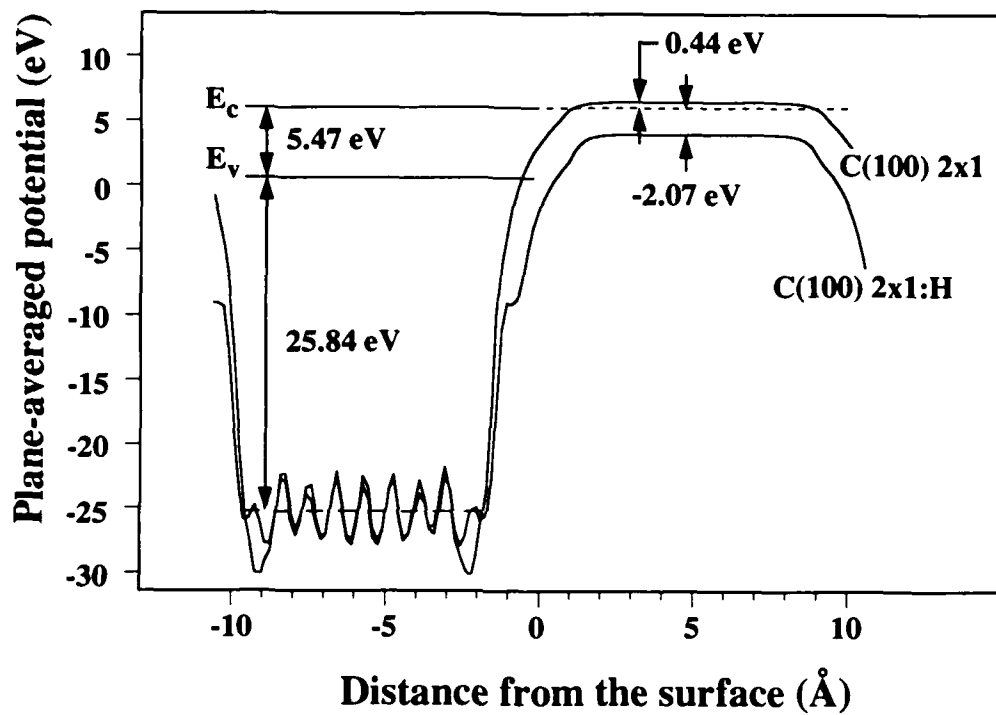
Fig. 3. Calculated plane-averaged, self-consistent potentials of a
hydrogen-free and monohydride terminated 2x1 reconstructed
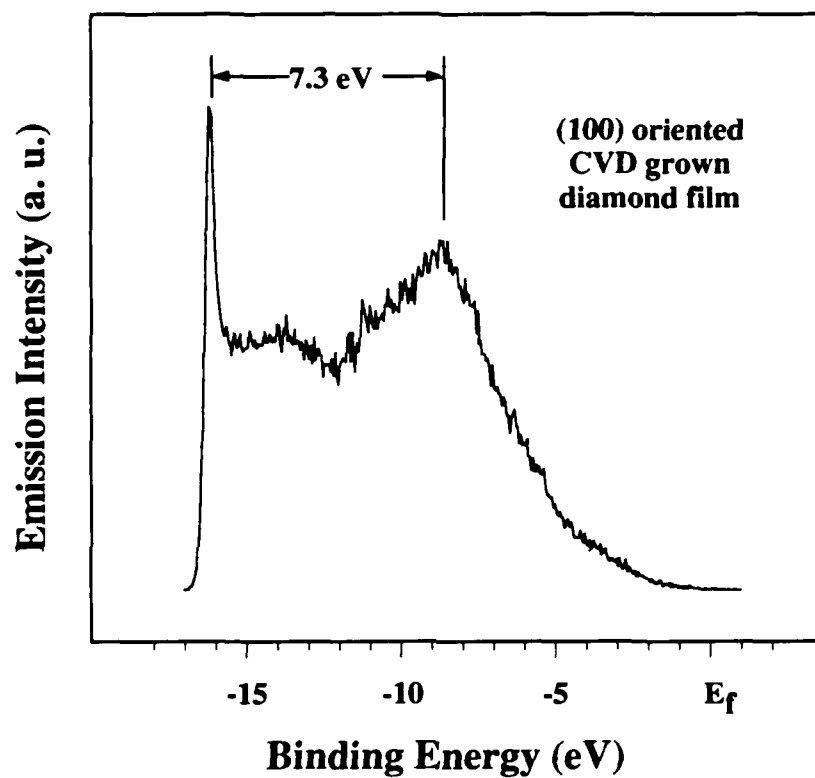diamond (100) surface.

Fig. 4. Photoemission obtained from a CVD grown, (100) oriented
diamond film indicates the presence of a negative electron affinity.

Distribution List

Mr. Max Yoder
Office of Naval Research
Electronics Program–Code 1114
800 North Quincy Street
Arlington, VA 22217

Office of Naval Research
Resident Representative
The Ohio State Univ. Research Center
1960 Kenny Road
Columbus, OH 43210-1063

Director
Naval Research Laboratory
Attention: Code 2627
Washington, DC 20314

Defense Technical Information Center
Building 5
Cameron Station
Alexandria, VA 22314

Robert J. Markunas
Research Triangle Institute
Post Office Box 12194
Research Triangle Park, NC 27709-2194

Dr. Ron Rudder
Research Triangle Institute
P. O. Box 12194
Research Triangle Park, NC 27709-2194

Howard Schmidt and Mark Hammond
Schmidt Instruments
2476 Bolsover, Suite 234
Houston, TX 77004

Prof. Karl Spear
Pennsylvania State University
201 Steidle
University Park, PA 16802

Michael W. Geis
Lincoln Laboratories
244 Wood Street
P. O. Box 73
Lexington, MA 02173

Professor R. F. Davis
Materials Science and Engineering
Box 7907
North Carolina State University
Raleigh, NC 27695-7907

Professor R. J. Nemanich
Department of Physics
Box 8202
North Carolina State University
Raleigh, NC 27695-8202

Professor R. J. Trew
Electrical and Computer Engineering
Box 7911
North Carolina State University
Raleigh, NC 27695-7911

Professor John C. Angus
Chemical Engineering
Case Western Reserve University
Cleveland, OH 44106

Dr. Andrzej Badzian
271 Materials Research Laboratory
The Pennslyvania State University
University Park, PA 16802

Dr. H. Liu
Emcore Corp.
35 Elizabeth Avenue
Somerset, NJ 08873

Prof. Karen Gleason
Chemical Engineering, Rm. 66-462
M. I. T.
Cambridge, MA 02134

Prof. Jerry Whitten
Chemistry
Box 8201
N. C. State University
Raleigh, NC 27695-8201

Dr. Ray Thomas
Research Triangle Institute
Box 12194
Research Triangle Park, NC 27709-2194

Allen R. Kirkpatrick
Epion Corp.
4R Alfred Circle
Bedford, MA 01730

Robert C. Linares
Linares Management Assoc., Inc.
P. O. Box 336
Sherborn, MA 01770

Dr. Martin Kordesch
Physics
Clippinger Research Laboratories
Ohio University
Athens, OH 45701-2979

Prof. Charter Stinespring
Chemical Engineering, Box 6101
West Virginia University
Morgantown, WV 26506

Robert Hauge
Chemistry
Rice University
Houston, TX 77251

Dr. John Margrave
HARC
4800 Research Forest Drive
The Woodlands, TX 77381

Dr. John Posthill
Research Triangle Institute
P. O. Box 12194
Research Triangle Park, NC 27709-2194

Dr. James Butler
NRL Code 6174
Washington, DC 20375

Dr. Andrew Freedman
Aerodyne Research, Inc.
45 Manning Road
Billerica, MA 01821

Prof. Michael Frenklach
Penn State University
202 Academic Projects Bldg.
University Park, PA 16802

Prof. Jeffrey T. Glass
Materials Science & Engr.
Box 7907
North Carolina State University
Raleigh, NC 27695-7907

Dr. Warren Pickett
NRL Code 4692
Washington, DC 20375-5000

Prof. Max Swanson
Physics
University of North Carolina
Chapel Hill, NC 27599-3255

Dr. James Zeidler
Code 7601
NRaD
San Diego, CA 92152